Lack of immunological cross-reactivity between parasite-derived and recombinant forms of ES-62, a secreted protein of *Acanthocheilonema viteae*

C. A. EGAN[1], K. M. HOUSTON[1], M. J. C. ALCOCER[2], A. SOLOVYOVA[3], R. TATE[4], G. LOCHNIT[5], I. B. McINNES[6], M. M. HARNETT[6], R. GEYER[5], O. BYRON[3] *and* W. HARNETT[1]*

[1] *Department of Immunology, University of Strathclyde, Glasgow G4 0NR, UK*
[2] *Division of Nutritional Sciences, University of Nottingham, Loughborough LE12 5RD, UK*
[3] *Division of Infection and Immunity, Institute of Biomedical and Life Sciences, University of Glasgow G12 8QQ, UK*
[4] *Department of Physiology and Pharmacology, University of Strathclyde, Glasgow G4 0NR, UK*
[5] *Institute of Biochemistry, University of Giessen, Giessen D35392, Germany*
[6] *Division of Immunology, Infection and Inflammation, University of Glasgow, Glasgow G11 6NT, UK*

(*Received 21 June 2005; revised 23 August 2005; accepted 24 August 2005; first published online 11 October 2005*)

SUMMARY

The longevity of filarial nematodes is dependent on secreted immunomodulatory products. Previous investigation of one such product, ES-62, has suggested a critical role for post-translationally attached phosphorylcholine (PC) moieties. In order to further investigate this, ES-62 lacking PC was produced, using the *Pichia pastoris* recombinant gene expression system. Unlike parasite-derived ES-62, which is tetrameric the recombinant material was found to consist of a mixture of apparently stable tetramers, dimers and monomers. Nevertheless, the recombinant protein was considered to be an adequate PC-free ES-62 as it was recognized by existing antisera against the parasite-derived protein. However, subsequent to this, recognition of parasite-derived ES-62 by antibodies produced against the recombinant protein was found to be absent. In an attempt to explain this, recombinant ES-62 was subjected to structural analysis and was found to (i) contain 3 changes in amino acid composition; (ii) demonstrate significant alterations in glycosylation; (iii) show major differences in protein secondary structure. The effects of these alterations in relation to the observed change in immunogenicity were investigated and are discussed. The data presented clearly show that recognition by existing antibodies is insufficient proof that recombinant proteins can be used to mimic parasite-derived material in studies on nematode immunology and vaccination.

Key words: antigenic cross-reactivity, ES-62, filarial nematode, *Pichia pastoris*, protein folding, recombinant protein expression.

INTRODUCTION

There are 8 species of filarial nematodes known to infect humans, 3 of which, namely *Wuchereria bancrofti*, *Brugia malayi* and *Onchocerca volvulus* are responsible for much of the morbidity seen in the Tropics (WHO, 1997). Currently, it is estimated that 150 million people suffer from at least one of these named parasites with a further 1 billion at risk of infection, and symptoms range from skin lesions to elephantiasis and blindness. In general, the perspective of researchers is that filarial nematodes are able to modulate the host's immune system via the immunomodulatory excretery/secretory, or ES molecules they produce (for reviews see Harnett and Parkhouse, 1995; Maizels, Blaxter and Scott, 2001), leading to the long life-span observed in the worms, which can be in excess of 5 years (Subramanian *et al*. 2004). Infected individuals have been shown to display immune responses deemed 'defective'. Although precise details of the alterations have yet to be agreed on, the general profile seen, especially in asymptomatic patients is consistent with a Th-2 – like immunological phenotype. All subclasses of IgG are down regulated with the exception of IgG4 (Ottesen *et al*. 1985; Kurniawan *et al*. 1993), which is not a very useful antibody as IgG4 is frequently monovalent, unable to activate complement or bind macrophages with high affinity. Regarding cytokine production, in the main there is an increase in IL-10 and a reduction in IFNγ levels (reviewed by Lawrence, 2001).

ES-62 is a well-characterized secreted immunomodulatory molecule, first discovered in *Acanthocheilonema viteae*, a filarial nematode of the gerbil, 15 years ago (Harnett *et al*. 1989).

* Corresponding author: Department of Immunology, Strathclyde Institute for Biomedical Sciences, University of Strathclyde, Glasgow G4 0NR, UK. Tel: +44 141 548 3725. Fax: +44 141 548 3427. E-mail: w.harnett@strath.ac.uk

Parasitology (2006), **132**, 263–274.
doi:10.1017/S0031182005009005 Printed in the United Kingdom

Homologues of ES-62 have been found in *B. malayi* and *O. volvulus* (Harnett, Harnett and Byron, 2003), making the study of this molecule and its effects on the immune system prudent. As the name suggests, ES-62 has a molecular mass of approximately 62 kDa when analysed by SDS-PAGE under reducing and denaturing conditions (Harnett *et al*. 1989), though later it was shown that the molecule exists as a tetramer in its excreted form (gel filtration (Harnett *et al*. 1993) and sedimentation equilibrium analysis (Ackerman *et al*. 2003)).

Many of the immunological effects exerted by ES-62 can be attributed to the phosphorylcholine (PC) moiety, (reviewed by Harnett and Harnett, 2001) which is found attached to N-linked carbohydrate chains (Harnett *et al*. 1993). Thus, much of ES-62's activity can be mimicked by PC conjugated to proteins such as albumin including effects on B cells (Harnett and Harnett, 1993), T cells (Harnett *et al*. 1999) and macrophages (Goodridge *et al*. 2004). In order to further investigate PC's role in ES-62's immunomodulatory activities, ES-62 lacking PC was produced using inhibitors of enzymes involved in N-linked oligosaccharide processing or phosphorylcholine synthesis (Houston, Cushley and Harnett, 1997, Houston and Harnett, 1999*b*). However, although some work was carried out using this material (Houston *et al*. 2000) the methods used to produce the PC-free ES-62 were ultimately found to be too inconsistent with respect to efficacy to warrant routine application. As an alternative we have produced PC-free ES-62 as a recombinant protein in the yeast *Pichia pastoris*, which does not contain the machinery necessary to post-translationally add PC to secreted proteins. We now show that in spite of the recombinant material being initially recognized by antibodies directed against the parasite-derived protein, it turns out to have virtually no immunological cross-reactivity with the latter and the reasons for this are explored.

MATERIALS AND METHODS

Parasite-derived material

ES-62 was purified from spent culture medium of adult *Acanthocheilonema viteae* by ultrafiltration as described previously (Wilson *et al*. 2003).

Media and reagents for Pichia pastoris

The media and reagents used were as described previously (Alcocer *et al*. 2002). Briefly, *P. pastoris* GS115 (Invitrogen) was maintained in yeast extract peptone dextrose (YPD) broth (Difco). Minimal dextrose (MD) plates were used for plasmid selection, buffered minimal glycerol (BMG) broth for enrichment and buffered minimal methanol (BMM) broth for induction.

Construction of expression plasmids

The ES-62 gene (Harnett *et al*. 1999) was amplified by PCR using the primers: MJA121 5′-AAGGGGTATCTCTCGAGAAAAGAGAGGCAGCTGTCCTTCCGGACAAAACTGTCGCT3′ and MJA122 5′-ATGGGAATTCTTATAGCTTTTTACGATCAGATTTCTCAGTAGT3′ with 35 cycles of 94 °C 30 s, 54 °C 30 s, 72 °C 90 s, using Amplitaq (2 U/100 μl; Applied Biosystems) according to the manufacturer's instructions. The PCR product (ca. 1500 bp) was gel-purified, digested with *Eco* RI/*Xho* I enzymes for 4 h at 37 °C and ligated into pPIC9 (Invitrogen) previously digested with the same enzymes. The resulting plasmids were transformed into *E. coli* XL1Blue (Stratagene) and selected under ampicillin (100 μg/ml) according to standard protocols (Ausubel *et al*. 2001). Plasmids containing the inserted gene were purified (midi kit – Qiagen) and sequenced using the Sanger method with dye terminators (Applied Biosystems).

Transformation and expression in P. pastoris

pPIC9-derived plasmids containing ES-62-encoding sequences were linearized at the *Sal* I site for 4 h at 37 °C. The linearized plasmids were then transformed into *P. pastoris* GS115 (5 μg/transformation) and the transformed strains were selected on MD plates following electroporation according to the manufacturer's instructions (Invitrogen). Clones able to grow in the absence of histidine were inoculated into a sterile 96-well plate format containing BMG and incubated overnight at 30 °C. The 96 clones were then expanded to 4 × 24-well plates containing BMG (1·5 ml/well) and incubated overnight at 30 °C. After centrifugation (750 ***g*** for 15 min), the 24-well plates were emptied by suction and BMM broth (containing methanol at 0·5% v/v) added. Expression was allowed to take place in an orbital shaker (200 rpm) for 48 h with addition of methanol (0·5% v/v) every 12 h. After induction with methanol, the 4 × 24-well plates were centrifuged (750 ***g*** for 15 min) and the supernatant (500 μl) transferred under vacuum to a wetted PVDF (Millipore) membrane in a dot blot format system. The membrane was then blocked by incubation with 10 ml of BSA (bovine serum albumin, 5% w/v) in TBS (Tris-Buffered Saline, 20 mM Tris pH 7·5, 0·9% (w/v) sodium chloride) for 1 h. All incubations were performed at 37 °C in a standard hybridization oven. After 3 washes (5 min each) with TBST (TBS plus Tween 20–0·1% v/v), the membranes were incubated for 2 h with KK6, a mouse monoclonal antibody that recognizes a conformational epitope on ES-62 (Stepek *et al*. 2002) diluted (1 : 1000) in TBST plus 20% (v/v) of *P. pastoris* supernatant extract that was previously prepared and did not contain the target protein. The membrane was then washed

https://doi.org/10.1017/S0031182005009005 Published online by Cambridge University Press

3 times with TBST and incubated for a further 1 h with the secondary HRP-labelled anti-mouse IgG, diluted 1 : 20000 in TBST. After the 3 washes with TBST the membrane was incubated with nitroblue tetrazolium and 5-bromo-4-chloro-3-indolyl phosphate toluidine substrate. Once the reaction was completed, the blot was washed with distilled water and dried. Analysis revealed that most of the wells in the culture plate contained recombinant ES-62.

Large-scale production of recombinant ES-62

A positive clone was selected and grown at high density ($OD_{600\ nm}$ 3–6) in 2 × 2 l flasks with Minimal Media containing Glycerol (MMG) at 28 °C with agitation. The culture was then centrifuged (1200 rpm for 10 min) and the pellet re-suspended in Minimal Media with Methanol (MMM) and incubated with agitation (200 rpm) at 28 °C for 48–72 h with the addition of methanol to a final concentration of 0·5% (v/v) every 24 h. After induction, the supernatant was separated from the cells by centrifugation (1200 rpm for 10 min) and filtered through a 0·22 μm membrane. The supernatant was then concentrated and the salt eliminated by buffer exchange (PBS pH 7·4) using a tangential flow system (Vivascience, molecular weight cut-off 100 000). The sample was then further concentrated using Amicon centricon tubes with a 100 000 cut-off membrane. Finally, the sample was assayed for protein content using the Bio-Rad protein assay reagent and then stored at −20 °C in 10% glycerol/0·01 M magnesium sulphate.

Site directed mutagenesis of intact plasmids

In order to introduce point mutation on the pPIC9 based constructs, the general procedure described by Chen and Ruffner (1998), with minor modifications, has been followed. Essentially two 5′ phosphorylated primers complementary to different strands and separated by 300 bp between the 3′ ends were used. One of the primers carried the inserted mutation. The reaction mixture (50 μl) contained 10 ng of native plasmid, 10 pmol of each primer, 10 nmol of dNTPs, 5 nmol of ATP, 2·5 U *Pfu* DNA polymerase (Stratagene, La Jolla, CA), 4 U *Pfu* DNA ligase (Stratagene), in 1 ml of cloned *pfu* DNA polymerase reaction buffer consisting of 20 mM Tris-HCl (pH 8·8), 10 mM KCl, 10 mM $(NH_4)_2SO_4$, 2 mM $MgSO_4$, 1% Triton X-100 and 100 μg/ml BSA. The mixture was pre-incubated at 70 °C for 10 min allowing the ligase to repair any nicks in the template. It was then subjected to thermal cycling at 95 °C for 10 s (denaturation), 50 °C for 30 s (annealing), 72 °C for 17 min (extension), 95 °C for 10 s (denaturation) and 72 °C for 17 min (annealing, extension and ligation) for 20 cycles. The amplified plasmid was then digested with *Dpn*I restriction enzyme (10 U) in the same PCR buffer at 37 °C for 2 h in order to remove the starting template DNA and subsequently introduced into *Escherichia coli* strain DH5[α] by electroporation. After ampicillin selection the transformed clones were amplified and sequenced following standard techniques.

SDS-PAGE/Western blotting and dot blotting

SDS-PAGE and Western analysis were performed according to the manufacturer's instructions (on some occasions NOVEX – Invitrogen, on others Bio-Rad), using Immobilon PVDF membrane (Millipore), or Hybond-C (Amersham). Rabbit anti-ES-62 serum and $TEPC_{15}$, a myeloma protein that recognizes PC, were used as primary antibodies and appropriate enzyme-conjugated antisera as detection systems as described previously (Harnett *et al*. 1993). Dot blotting was undertaken using similar procedures with the monoclonal antibody KK6 referred to earlier.

Inoculation of mice

Balb/c mice were bred at the University of Strathclyde, and used at 6–8 weeks of age. Three groups of 5 female Balb/c mice received weekly subcutaneous injections of 2 μg per animal of either native ES-62 or recombinant ES-62 (rES-62). Weekly serum samples were taken and antibody levels to ES-62 and rES-62 measured by ELISA.

ELISA

The 96-well plates were coated with 100 μl of phosphate-buffered saline (PBS) containing parasite-derived ES-62 or recombinant ES-62 at a concentration of 2 μg/ml overnight at 4 °C. After washing, the plates were blocked for 1 h at 37 °C with 4% bovine serum albumin (BSA) in PBS. The plates were then washed and duplicate samples of sera from the immunization study were added at a starting concentration of 1/100 and diluted 1/3 down the length of the plate in PBS containing Tween 20 (0·05% v/v) and the plates incubated for 1 h at 37 °C. After washing, wells were incubated with a 1/20 000 dilution of peroxidase-conjugated rabbit anti-mouse IgG1 or IgG2a for 1 h at 37 °C. The plates were washed once more and substrate added and the plates incubated at room temperature in the dark for 15 min to allow colour development. The reaction was stopped by the addition of 50 μl of H_2SO_4/well and the plate read at 450 nm. Data are expressed as reciprocal end-point dilutions, with error bars calculated by standard error of the mean.

Carbohydrate constituent analysis

Carbohydrate constituent analyses were carried out as detailed elsewhere (Geyer *et al*. 1982).

https://doi.org/10.1017/S0031182005009005 Published online by Cambridge University Press

Biophysical analysis

Circular dichroism (*CD*). Spectra of rES-62 were recorded at 20 °C using a Jasco J-600 spectropolarimeter (Jasco UK Ltd, UK). The far ultraviolet (UV) CD spectrum (260–190 nm) of rES-62 was measured using a 0·02 cm path-length quartz cell at a scan speed of 50 nm/min and a response of 0·5 s, 8 scans were taken. The near UV CD spectrum (320–260 nm) of rES-62 was obtained in the same cell at a scan speed of 20 nm/min and a response of 1 s, 4 scans taken. The protein concentration was 0·5 mg/ml in phosphate buffer (91·5 mM Na_2HPO_4, 58·5 mM NaH_2PO_4, pH 7·4). The circular dichroism spectra were analysed with the set of CD analysis programs available on the DICHROWEB web server (http://www.cryst.bbk.ac.uk/cdweb/html/) (Whitmore and Wallace, 2004). Secondary structure estimations were obtained using the Provencher and Glockner method (Provencher and Glockner, 1981).

Analytical ultracentrifugation (*AUC*). Sedimentation velocity (SV) and sedimentation equilibrium (SE) experiments were performed at 4 °C in a Beckman Coulter (Palo Alto, CA, USA) Optima XL-I analytical ultracentrifuge using both absorbance at 278 nm and interference optics. The partial specific volume ($\bar{v}$) for the protein part of rES-62 was calculated from its amino acid sequence, using the program SEDNTERP (Laue *et al*. 1992). The contribution of the carbohydrate part was estimated using the following formula (Durchschlag, 1986)

$$\bar{v}_{complex} = \frac{\bar{v}_p + \sum_i \delta_i \bar{v}_i}{1 + \sum_i \delta_i} \quad (1)$$

where $\bar{v}_{complex}$, $\bar{v}_p$ and $\bar{v}_i$ are the partial specific volumes of the glycosylated the protein, protein part alone and the carbohydrate part respectively; δ_i is the amount of carbohydrate in grams per gram of protein. The partial specific volume for the glycosylated form of rES-62 was calculated using values valid for a temperature of 20 °C and then extrapolated to the experimental temperature following the method of Durchschlag (1986)

$$\bar{v}_T = \bar{v}_{20} + 4{\cdot}25 \times 10^{-4}(T - 293{\cdot}15) \quad (2)$$

where T is the experimental temperature (K).

The density and viscosity of PBS buffer at the experimental temperature was calculated using SEDNTERP. The distribution of sedimenting material was modelled as a distribution of Lamm equation solutions (Schuck, 2000) where the measured boundary a(r, t) was modelled as an integral over the differential concentration distribution c(s).

$$a(r, t) = \int c(s)\chi(s, D, r, t)ds + \varphi \quad (3)$$

where φ is a noise component, r is the distance from the centre of rotation and t is time. The expression χ(s, D, r, t) denotes the solution of the Lamm equation for a single species (Lamm, 1929) by finite element methods (Schuck, 1998). Implemented in the program SEDFIT (www.analyticalultracentrifugation.com) the integral Eq. 3 is solved numerically by discretisation into a grid of 150 sedimentation coefficients for interference data and 200 coefficient for absorbance data and the best-fit concentrations for each plausible species are calculated via a linear least squares fit. The sedimentation velocity profiles were fitted using a maximum entropy regularisation parameter of $p = 0{\cdot}95$. This model was applied to describe the heterogeneity of the material moving in the AUC cell. Also, SV boundaries were treated as comprising discrete independent species for the exact determination of sedimentation coefficients (s) for the species observed. Sedimentation coefficients were extrapolated to zero concentration and converted to standard conditions: those that would be measured at 20 °C in water.

Equilibrium in SE experiments was attained after 45 h. The speeds of rotation were selected so that the value for the parameter σ (the reduced apparent molecular weight) (Yphantis, 1960) was between 2 and 4 for each plausible oligomeric species. Thus, SE traces for rES-62 were obtained at 8000 rpm, 11 500 rpm, 16 500 rpm, 20 000 rpm and 23 000 rpm. True optical baselines were obtained after a further 6 h of rotation at 48 000 rpm again. The concentration of samples in the SE experiments ranged between 1·5 μM and 23 μM of rES-62 monomer. SE data were fitted globally using the Beckman XL-A – XL-I software implemented in Microcal ORIGIN 6.0 and the NONLIN program (Johnson *et al*. 1981) (WINDOWS version) and also the program SEDPHAT (www.analyticalultracentrifugation.com) (Schuck, 2004).

Small-angle X-ray scattering. rES-62 was extensively dialysed against PBS buffer prior to small-angle x-ray scattering experiments. Concentrated rES-62 was microfuged (20 800 ***g***) for 20 min and then transferred into a capillary and placed in the SAXS beamline at the ELLETRA synchrotron (Trieste, Italy) with an electron energy of 2 GeV and a wavelength of 1·5 Å. Two camera lengths were used in the experiments: 1·5 m to cover a momentum transfer range of $0{\cdot}01 < s < 0{\cdot}3$ Å^{-1} and 0·8 m for $0{\cdot}1 < s < 0{\cdot}5$ Å^{-1}, where $s = (4\pi\sin\theta)/\lambda$ and 2θ is the scattering angle. The 1D detector was calibrated using a sample of silver bionate. For the short camera length the concentration of the protein was 10 mg/ml while for the long camera length the sample concentration was 7 mg/ml. Experimental data were collected and averaged as 30 × 60 sec frames for both camera lengths. The data were normalized for buffer

https://doi.org/10.1017/S0031182005009005 Published online by Cambridge University Press

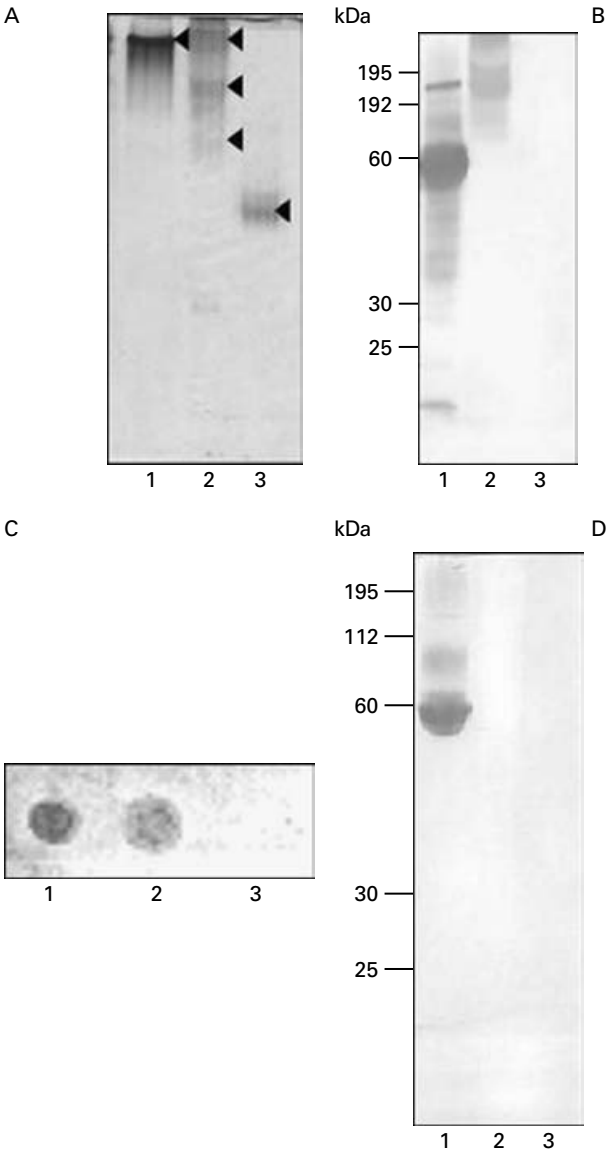

Fig. 1. (A) PAGE of parasite-derived and recombinant ES-62: 2·5 μg of parasite-derived (lane 1), and recombinant ES-62 (lane 2) with ovalbumin (lane 3) as a control were run on 12% polyacrylamide gels under non-reducing, non-denaturing conditions. The gels were fixed and stained with Sigma Brilliant Blue Colloidal-G Stain. The solid arrows indicate ES-62 (lane 1), rES-62 (Lane 2) and ovalbumin. (B) SDS-PAGE/Western blotting of parasite-derived and recombinant ES-62 with polyclonal rabbit anti-ES-62 serum: 2·5 μg of parasite-derived (lane 1), and recombinant ES-62 (lane 2) with ovalbumin (lane 3) as a control were run on 12% polyacrylamide gels under reducing, denaturing conditions. The polypeptides were transferred to a nitrocellulose membrane and then probed with a polyclonal rabbit anti-ES-62 serum followed by an anti-rabbit horseradish peroxidase-conjugated secondary antibody. Molecular weight markers (kDa) are indicated on the left of the gels. (C) Dot-blot analysis of parasite-derived and recombinant ES-62 with a monoclonal anti-ES-62 antibody: 1·25 μg of parasite-derived (lane 1), and recombinant ES-62 (lane 2) with ovalbumin as a control (lane 3) were placed on nitrocellulose Hybond-C (Amersham) and analysed by dot blot using a monoclonal anti-ES-62 antibody directed against a conformational epitope on the parasite-derived ES-62 tetramer. (D) SDS-PAGE of parasite-derived and recombinant ES-62 with $TEPC_{15}$: 2·5 μg of parasite-derived (lane 1), and recombinant ES-62 (lane 2) with ovalbumin (lane 3) as a control were run on 12% polyacrylamide gels under reducing, denaturing conditions, transferred to a nitrocellulose membrane, then probed with $TEPC_{15}$ followed by an anti-mouse Ig horseradish peroxidase-conjugated secondary antibody. Molecular weight markers (kDa) are indicated on the left of the gel.

scattering and detector response using in-house software run on an IgorPro platform.

RESULTS

Oligomerization and antigenicity of recombinant ES-62

An advantage of employing the *Pichia pastoris* expression system to produce secreted proteins is that the very low level of additional protein secreted both by the yeast and present in the culture medium means that most of the protein present in the latter is the recombinant protein. We therefore adopted a very simple purification scheme, removing all proteins of molecular mass $<$100 kDa from the medium by ultrafiltration. The medium was then concentrated and the sample analysed by PAGE under non-reducing and non-denaturing conditions. Two major polypeptides were observed, both diffuse in nature, one migrating slightly more slowly than the native molecule and one rather faster (Fig. 1A). Two further minor bands of likely lower molecular mass were also observed, one surprisingly (given the purification system) migrating more rapidly than ovalbumin. Interestingly, unlike parasite-derived ES-62, which monomerizes (from a tetramer) when examined by SDS-PAGE under reducing conditions (see Fig. 1B), all 4 polypeptides present in the concentrated *Pichia* culture medium showed little evidence of a change in mass (result not shown). However, Western blotting using the rabbit polyclonal antiserum against ES-62, suggested that the 3 bands of higher molecular mass might correspond to recombinant ES-62 (Fig. 1B). It was thus tentatively considered that the recombinant molecule might consist of several forms corresponding in size to tetramers, dimers and monomers with the oligomers being stable structures not amenable to dissociation. Consistent with this it was found that the recombinant molecule could not be completely monomerized even after boiling for 10 min in the presence of mercaptoethanol. The changes in oligomerization and susceptibility to monomerization witnessed with the recombinant ES-62 raised the possibility that it might show some changes in conformation that could result in loss of peptide

https://doi.org/10.1017/S0031182005009005 Published online by Cambridge University Press

epitopes. However, when the recombinant material was re-analysed by dot blotting for interaction with KK6, the monoclonal antibody that recognizes a conformational epitope on the parasite-derived protein (Fig. 1C), binding was still clearly apparent. Finally, to confirm that the recombinant protein lacked PC it was analysed using $TEPC_{15}$, a myeloma-derived antibody directed against PC. It can be seen in Fig. 1D that only the wild-type protein is recognized by this antibody, confirming the absence of PC from the recombinant molecule.

Immunogenicity of recombinant ES-62

Recombinant ES-62 was injected into mice and serum samples taken and tested for antibodies against the recombinant and parasite-derived molecules by ELISA. The molecule was found to induce a strong IgG1 antibody response (Fig. 2A) but unlike PC-free ES-62 produced by earlier methods (Houston *et al*. 2000) no IgG2a (result not shown). To our surprise, the IgG1 antibodies produced completely failed to recognize the parasite-derived material (Fig. 2B). Likewise, antibodies generated against the parasite-derived material in mice completely failed to recognize the recombinant material (Fig. 2A and B). Antibody recognition of denatured forms of both proteins was investigated with both mouse sera to determine whether epitopes recognized were conformational. It appears that the parasite-derived ES-62 epitopes are mostly conformational in nature, as the recognition of the denatured parasite-derived protein was greatly reduced, relative to the non-denatured (Fig. 2C). However, antibody interaction with the denatured rES-62 appears to be essentially no different from that witnessed with the non-denatured rES-62 (Fig. 2D) suggesting that the epitopes recognized on the recombinant molecule are not conformational. There are several possible explanations for this difference. The recombinant material used to coat the ELISA plate may not have been fully denatured (see earlier), the epitopes recognized by the antiserum against the recombinant molecule may be largely carbohydrate in nature or peptide epitopes on the recombinant molecule are essential linear. To investigate these possibilities compositional, structural and biophysical analysis of recombinant ES-62 was undertaken.

Amino acid sequence and carbohydrate constituent analysis of recombinant ES-62

Complete sequencing of the recombinant cDNA clone revealed 3 base mismatches. This corresponded to 3 amino acid changes at positions 245 (G > D), 286 (K > E) and 346 (N > S) on the parasite-derived molecule (Harnett *et al*. 1999). Preliminary lectin-binding analysis suggested that the recombinant material had higher mannose content than the native material (result not shown). The recombinant material was thus subjected to carbohydrate constituent analysis and its carbohydrate content was found to be ~6% with virtually all of this being mannose. This compares with roughly 3% carbohydrate for the parasite-derived protein, which also has much less mannose as a percentage (Haslam *et al*. 1997).

Biophysical analysis

Secondary structure and folding of recombinant ES-62. There is a negative peak in the far UV CD spectrum of rES-62 between 230 nm and 200 nm with a minimum at around 218 nm corresponding to a n-π^* band (Fig. 3A, solid line). A further negative peak close to 209 nm can be deconvoluted from the data reflecting a $(\text{n-}\pi^*)_{\text{parallel}}$ transition which indicates that the protein has little α-helical content. Secondary structure estimations were obtained using the program CONTIN (Provencher and Glockner, 1981) since other programs such as SELCON3 (Sreerama and Woody, 1993) and CDSSTR (Hennessey and Johnson, 1981) failed to fit the data. The CONTIN procedure (Provencher and Glockner, 1981) gives secondary structure estimations of 10% α-helix, 39% β-sheet, 21% β-turn and 30% remainder. Comparing these results with the data obtained previously for parasite-derived ES-62 (40% α-helix, 16% β-sheet, 16% β-turn and 28% remainder) (Ackerman *et al*. 2003) (see Fig. 3A, dashed line) we can conclude that the recombinant material has refolded most of its α-helix structure to β-sheets/turns but retained the same amount of unordered structure.

The near UV CD spectrum shows that the aromatic residues are located in asymmetric environments characteristic of the tertiary structure of a folded protein. Tryptophan residues in folded proteins generally give peaks close to 290 nm; tyrosine and phenylalanine residues give rise to peaks between 275 and 282 nm and 255 nm and 270 nm respectively.

Recombinant ES-62 was examined for heterogeneity using c(s) size-distribution analysis of sedimentation velocity (SV) data (Schuck *et al*. 2002). There were at least 3 peaks evident in the c(s) distribution pattern, with a major peak centred on an apparent sedimentation coefficient ($s^{app}_{20,w}$) of 5S and 2 less well-defined peaks at 3S and 8S (Fig 3B). Integration of the c(s) distribution for the 3 major peaks yielded the weight average sedimentation coefficient (s_w) for these species. The concentration dependence of s_w does not demonstrate the appearance of heavier species as concentration is increased but shows the expected concentration dependence of peak position: a movement towards lower s with increasing concentration (thermodynamic

https://doi.org/10.1017/S0031182005009005 Published online by Cambridge University Press

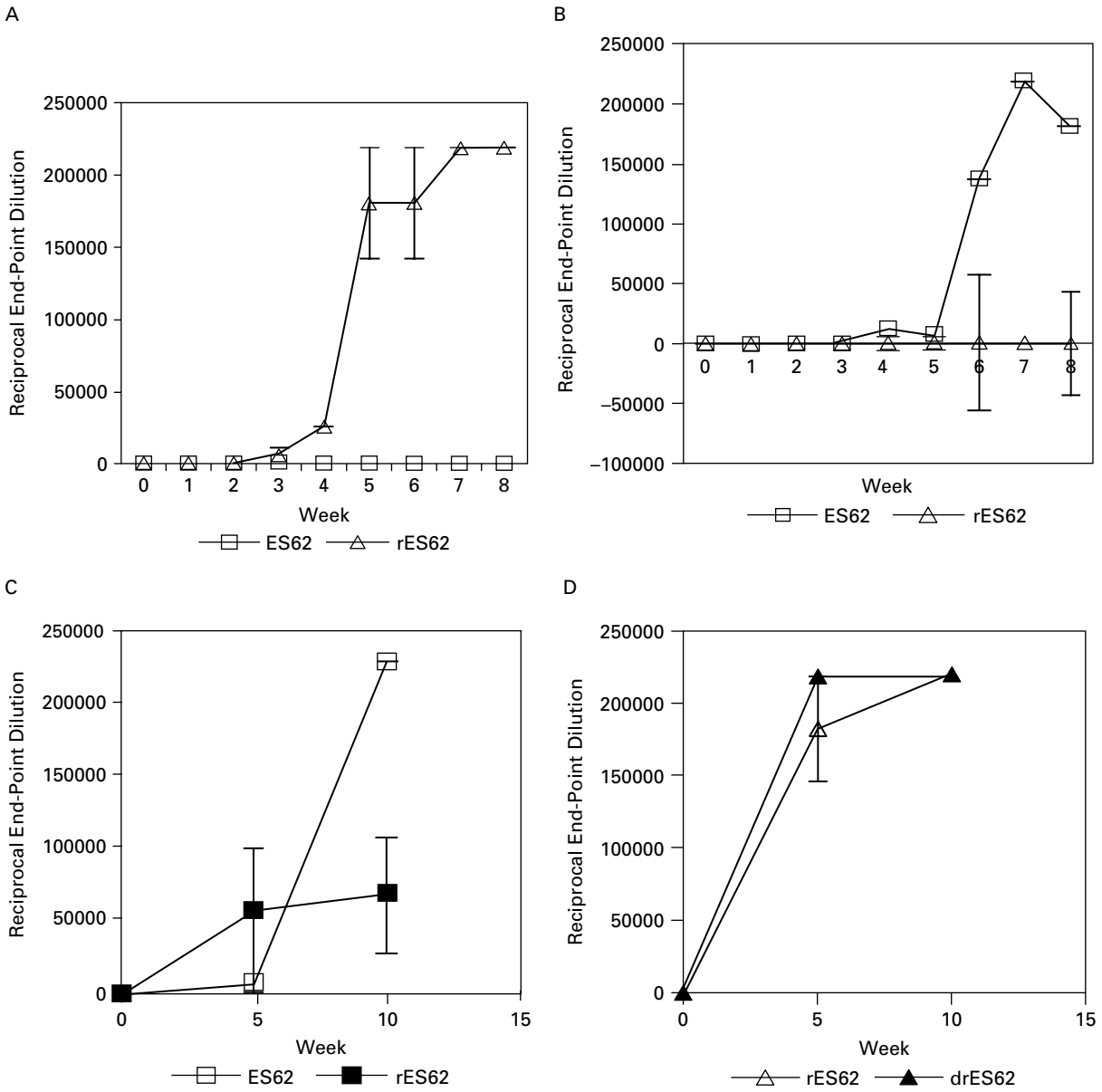

Fig. 2. (A) Recognition of recombinant ES-62 by IgG1 antibodies in serum of mice inoculated with recombinant or parasite-derived ES-62. Groups of 5 Balb/C mice were injected weekly with 2 μg parasite-derived (squares) or recombinant (triangles) ES-62 and serum samples taken. Samples were analysed by ELISA for recombinant ES-62 specific IgG1 responses in duplicate and mean values calculated ± standard error of the mean. Results are expressed as reciprocal end-point dilution. (B) Recognition of parasite-derived ES-62 by IgG1 antibodies in serum of mice inoculated with parasite-derived or recombinant ES-62. Groups of 5 Balb/C mice were injected weekly with 2 μg parasite-derived (squares) or recombinant (triangles) ES-62 and serum samples taken. Samples were analysed by ELISA for parasite-derived ES-62 specific IgG1 responses in duplicate and mean values calculated ± standard error of the mean. Results are expressed as reciprocal end-point dilution. (C) Recognition of denatured parasite-derived ES-62 by IgG1 antibodies in serum of mice inoculated with parasite-derived ES-62. Groups of 5 Balb/C mice were injected weekly with 2 μg parasite-derived ES-62 and serum samples taken. Samples were analysed by ELISA for denatured (filled squares) and non-denatured (open squares) parasite-derived ES-62 specific IgG1 responses in duplicate and mean values calculated ± standard error of the mean. Results are expressed as reciprocal end-point dilution. (D) Recognition of denatured recombinant ES-62 by IgG1 antibodies in serum of mice inoculated with recombinant ES-62. Groups of 5 Balb/C mice were injected weekly with 2 μg recombinant ES-62 and serum samples taken. Samples were analysed by ELISA for denatured (filled triangles) and non-denatured (open triangles) recombinant ES-62 specific IgG1 responses in duplicate and mean values calculated ± standard error of the mean. Results are expressed as reciprocal end-point dilution.

non-ideality). Therefore any redistribution between the rES-62 oligomeric species was not observed over the >10-fold concentration range examined, suggesting that the system is not in thermodynamic equilibrium, but instead comprises discrete independent oligomers.

https://doi.org/10.1017/S0031182005009005 Published online by Cambridge University Press

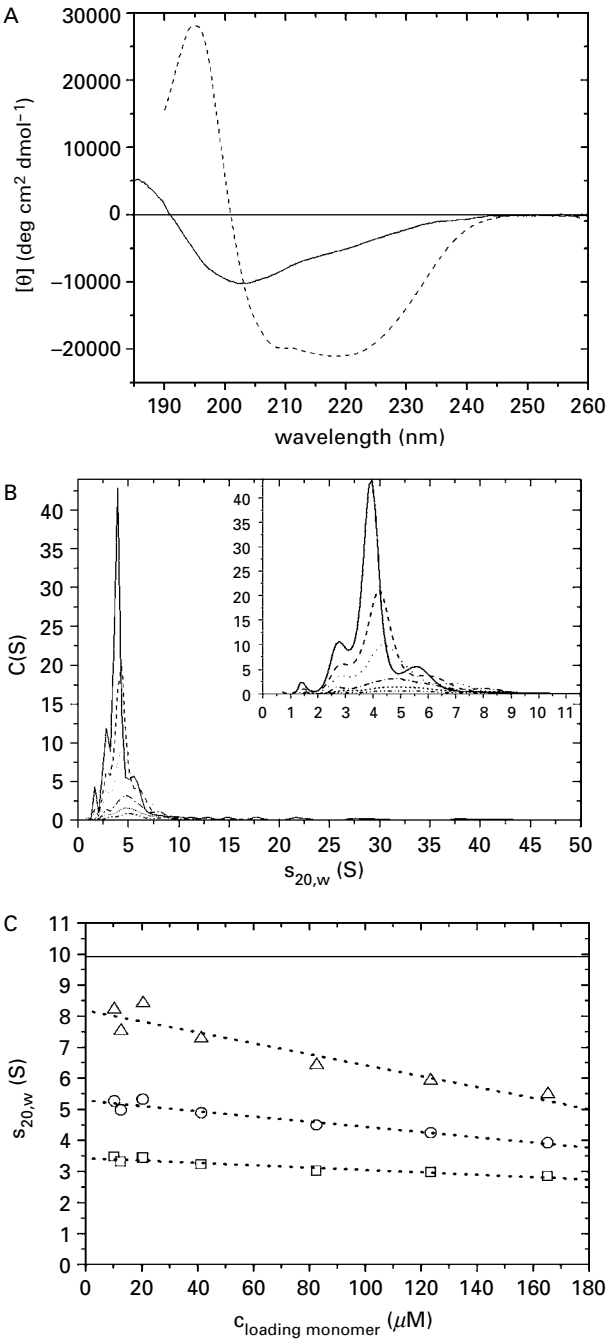

Fig. 3. Circular dichroism and sedimentation velocity characterization of rES-62. (A) Far UV circular dichroism spectrum for rES-62 (solid line) and parasite-derived ES-62 (dashed line) in phosphate buffer (91·5 mM Na_2HPO_4, 58·5 mM NaH_2PO_4, pH 7·4). The spectra were normalized for concentration. (B) Size distribution c(s); interference data obtained for monomeric loading concentrations of 165 μM (*solid line*) 123 μM (*dashed line*) 82 μM (*dotted line*) 41 μM (*dashed-dotted line*) 12 μM (*short dashed line*) 10 μM (*dashed-dotted-dotted line*). (C) The concentration dependence of s: 'monomer' (squares), 'dimer' (circles), 'tetramer' (triangles). The horizontal solid line marks the sedimentation coefficient obtained experimentally for parasite-derived ES-62 (Ackerman *et al*. 2003); dotted lines are the linear extrapolation of $s_{20,w}$ to zero concentration for the 3 species.

Direct fitting of SV boundaries gave sedimentation coefficients at infinite dilution and under standard conditions ($s^0_{20,w}$) of 3·4, 5·3 and 8·2 S (Fig. 3C) with good fits to the experimental data (not shown). The 3 species could be monomeric, dimeric and tetrameric rES-62. In order to compare these findings with the results for parasite-derived ES-62 (Ackerman *et al*. 2003), the value of the sedimentation coefficient for tetrameric parasite-derived ES-62 was deconvoluted to possible sedimentation coefficients for monomeric and dimeric species assuming that the oligomerization occurs 'side-to-side'. The data in Table 1 show the sedimentation coefficients for each oligomer from the recombinant material and the 'deconvoluted' s for parasite-derived ES-62. The fact that s for each oligomer of rES-62 is much less than that estimated for the parasite-derived counterpart implies rES-62 is more elongated/asymmetric than the parasite-derived protein.

The weight average molecular weight for rES-62 in solution was found at different rotation speeds in a sedimentation equilibrium experiment (data not shown). Thus, at a low rotation speed of 8000 rpm the weight average molecular mass (264 ± 50 kDa) was above the expected molecular mass for rES-62 tetramer (233 kDa) suggesting the presence of higher molecular weight aggregates. As the speed of rotation was increased the average molecular weight decreased reflecting a mixture of monomers and dimers (81 ± 13 kDa). The SE scans were treated using the equilibrium dissociation model, which did not give a significant improvement in fit to the data. Therefore we can conclude that these species are not undergoing equilibrium dissociation but exist independently, in agreement with the findings from SV experiments.

Small angle scattering. rES-62 scattered X-rays very well in solution, but significant differences between the parasite-derived and recombinant protein were observed. The overall shape of the rES-62 scattering curve is typical of that from very elongated particles (Volkov and Svergun, 2003). This is in contrast with parasite-derived ES-62, which is a rather globular particle (Ackerman *et al*. 2003). Since the AUC data have demonstrated clearly that rES-62 is very heterogeneous in solution it is not possible to use existing software routines for the determination of a solution structure for this kind of sample. At present we can reach only qualitative conclusions about rES-62 in solution.

Effects of changes in glycosylation on oligomerization and antigenicity of recombinant ES-62

Mature parasite-derived ES-62 has 4 potential N-type glycosylation sites, although structural analysis of peptides derived from the molecule suggests that the one closest to the C-terminus (amino

https://doi.org/10.1017/S0031182005009005 Published online by Cambridge University Press

Table 1. Sedimentation coefficients for ES-62 extrapolated to zero concentration and corrected to standard conditions

Species	$s^0_{20,w}$ for ES-62 (S)	
	Recombinant protein	Estimated from the parasite-derived ES-62 (tetramer) (Ackerman *et al*. 2003) assuming 'side-to-side' oligomerization
'Monomer'	3·4 ± 0·03	4·38
'Dimer'	5·3 ± 0·05	6·57
'Tetramer'	8·23 ± 0·15	9·85

acid position 381) is not utilized (unpublished result). In an attempt to investigate the effect of glycosylation on the structure and antigenicity of recombinant ES-62 three mutants were prepared each lacking 1 of the 3 remaining N-type glycosylation sites. Such treatment was found to have no effect on oligomerization of the mutants as each consisted of a mixture of monomers, dimers and tetramers as observed with the non-mutated recombinant material (Fig. 4A). Furthermore, each was recognized by the murine antiserum against the recombinant but not the parasite-derived material (Fig. 4B).

Effects of changes in amino acid composition on oligomerization and antigenicity of recombinant ES-62

To investigate the effect of the 3 amino acid changes, a new clone – rES-62 (II) was selected that was shown to be mutation-free by complete sequence analysis. Analysis of the recombinant protein by non-denaturing PAGE revealed the same pattern of bands as observed for the original recombinant protein (Fig. 5A). Furthermore, this protein was recognized by murine antibodies raised against the original recombinant protein, rES-62 (I) but not by antibodies raised against the parasite-derived protein (Fig. 5B).

DISCUSSION

The *Pichia pastoris* recombinant protein expression system was considered as a method for producing PC-free ES-62 for two reasons. First, it was considered unlikely that *P. pastoris* would possess the biochemical machinery to transfer PC to N-type glycans as to date it has only been observed in nematodes. Second, it was thought that the system would resolve the problem of unreliable efficacy associated with previously described methods (e.g. Houston and Harnett, 1999*a*). Both of these predictions turned out to be accurate as an adequate supply of PC-free material was readily produced. Although not all of the recombinant material was able to tetramerize, it reacted strongly with a monoclonal antibody against a conformational epitope on the parasite-derived ES-62 providing encouragement for the view that the molecule was likely to be more or less normally folded.

It was therefore surprising to find that antibodies generated against recombinant ES-62 in mice completely failed to recognize the parasite-derived material. Likewise polyclonal antisera generated against parasite-derived ES-62 in mice at the same time showed virtually no reactivity for the recombinant material. Biophysical analysis indicated that the latter showed features of a tertiary protein structure but that a significant portion of its secondary structure had been converted from α-helix to β-sheet. This will result in an overall change in shape for the recombinant protein and this was also predicted from the biophysical analysis. Furthermore, some of the recombinant material appeared to exist as stable monomers and dimers and these could lack secondary structural features stabilized by tetramerization. Further analysis by ELISA suggested that whereas the majority of antibodies induced by parasite-derived ES-62 recognized conformational peptide epitopes this was not true of the recombinant molecule. Thus, overall, the lack of immunological cross-reactivity between the 2 molecules may be due to the recombinant material having a less folded structure than the parasite-derived material. It certainly does not appear to be simply denatured: the murine anti-recombinant ES-62 antibody completely fails to recognize denatured parasite-derived ES-62 (results not shown).

The contribution to altered immunogenicity of the 2 changes in composition of the recombinant ES-62 was investigated. DNA sequencing of the recombinant clone had been undertaken at the beginning of the project to confirm identity but only at the N-terminal and hence the 3 base mutations were unknown. Unfortunately each of these resulted in a change in amino acid and equally unfortunate, in each case the change was not to a similar category of amino acid. Furthermore, each of the 3 amino acids in parasite-derived ES-62 obtained from *A. viteae* is conserved in ES-62 derived from *B. malayi* (77% conservation overall: Goodridge *et al*. 2005) raising the possibility that they could be important in correct protein folding. Certainly one of them – K^{286} is in a predicted region of α-helix (Ackerman *et al*. 2003) and also of note is that G^{245} is present in a region of the parasite-derived protein that shows homology to leucine-rich repeats that could conceivably be involved in protein dimerization. Nevertheless, when we came to examine a recombinant clone whose amino acid sequence was equivalent to that of the parasite-derived ES-62 it behaved in the same manner as the original recombinant clone with respect to oligomerization and antigenicity. Consistent with this, the total of the 3 changes was found to have

https://doi.org/10.1017/S0031182005009005 Published online by Cambridge University Press

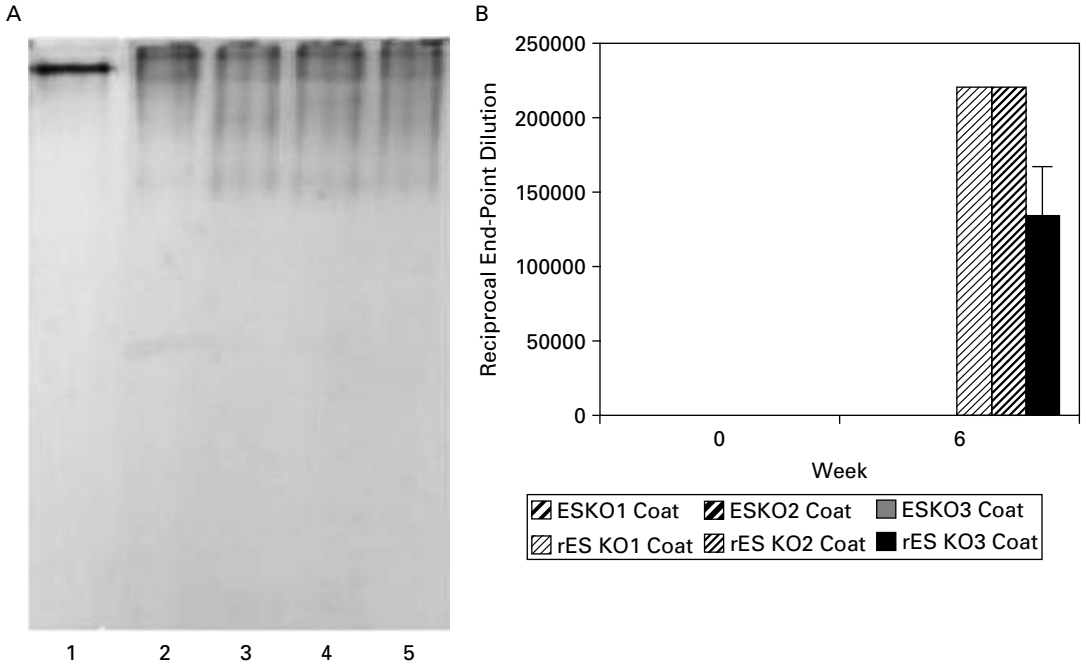

Fig. 4. (A) PAGE of recombinant ES-62 and N-type glycosylation site knock-out rES-62 mutants: 2·5 μg of parasite-derived ES-62 (lane 1), recombinant ES-62 (lane 2), N-type glycosylation site 1 (a.a. 194) knock-out (lane 3), N-type glycosylation site 2 (a.a. 235) knock-out (lane 4), N-type glycosylation site 3 (a.a. 325) knock-out (lane 5), were run on 12 % polyacrylamide gels under non-reducing, non-denaturing conditions. The gels were fixed and stained with Sigma Brilliant Blue Colloidal-G Stain. (B) Recognition of recombinant ES-62 lacking N-type glycosylation sites by IgG1 antibodies in serum of mice inoculated with parasite-derived or recombinant ES-62. Groups of 5 Balb/c mice were injected weekly with 2 μg parasite-derived or recombinant ES-62 and serum samples taken. Samples were analysed by ELISA for each of 3 distinct N-type glycosylation site knock-out rES-62 mutant recognition by IgG1 antibodies in duplicate and mean values calculated $\pm$ standard error of the mean. Results are expressed as reciprocal end-point dilutions.

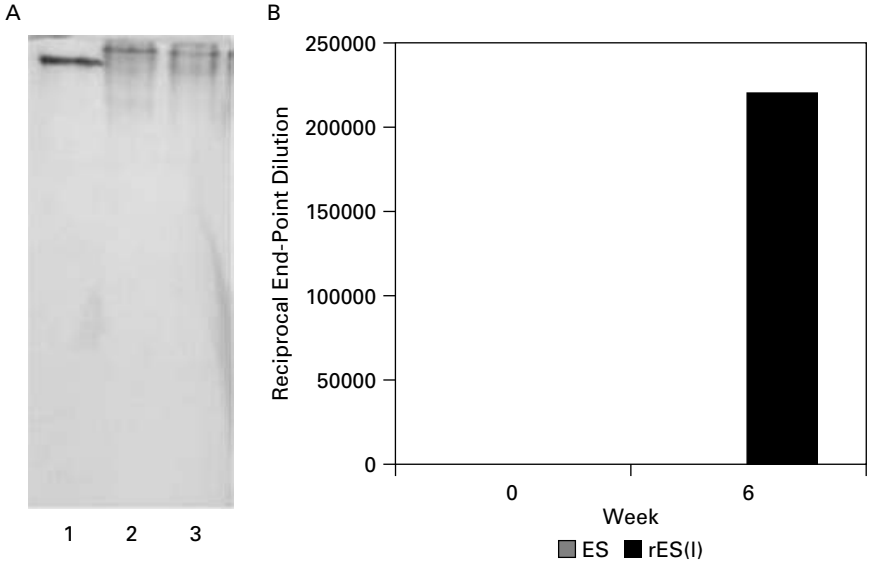

Fig. 5. (A) PAGE of recombinant ES-62 (I) and recombinant ES-62 (II): 2·5 μg of parasite-derived (lane 1), recombinant ES-62 (I) (lane 2), and recombinant ES-62 (II) (lane 3) were run on 12 % polyacrylamide gels under non-reducing, non-denaturing conditions. The gels were fixed and stained with Sigma Brilliant Blue Colloidal-G Stain. (B) Recognition of recombinant ES-62 (II) by IgG1 antibodies in serum of mice inoculated with parasite-derived or recombinant ES-62. Groups of 5 Balb/c mice were injected weekly with 2 μg parasite-derived or recombinant ES-62 (I) and serum samples taken. Samples were analysed by ELISA for rES-62 (II) specific IgG1 responses in duplicate and mean values calculated $\pm$ standard error of the mean. Results are shown as reciprocal end-point dilutions.

https://doi.org/10.1017/S0031182005009005 Published online by Cambridge University Press

very little effect on overall predicted secondary structure when this was assessed (result not shown). Regarding glycosylation, it had been expected that there would be an increase in mannose content typical of *Pichia* (Grinna and Tschopp, 1989) at the expense of complex glycan formation although the latter is fairly minimal in ES-62 in any case (Haslam *et al*. 1997). What was clear, however, was that there had been significant increase in the *extent* of glycosylation with the implication that much larger glycan chains would be present. What effect this would have on ES-62 structure is uncertain but it is known that glycosylation of proteins may stabilize secondary structure elements. We attempted to examine this by mutating distinct N-type glycosylation sites. This, however, had no effect on oligomerization or antigenicity with respect to the 3 mutants. We considered knocking out 2 or even all 3 glycosylation sites and measuring the effect of this but our previous experience of attempting to express ES-62 in *E. coli* suggested that the material could be insoluble (unpublished results). A further possibility could be to trim the glycans using mannosidases. At present, however, we cannot explain the changes in structure in terms of changes in carbohydrate or mutations in the amino acid sequence.

A question that remains is why the recombinant ES-62 is recognized by the monoclonal antibody KK6 given the apparent lack of cross-reactivity shown in the ELISA study. The most obvious explanation for this is that antibodies against this epitope represent a very minor component of the response to both forms of ES-62. It is also of interest that the recombinant ES-62 was ineffective in producing IgG2a antibodies, as PC-free ES-62 produced by other methods had been able to do this (Houston *et al*. 2000). This may suggest a difference in the way in which the 2 forms of the molecule interact with antigen presenting cells such as DCs and this is currently under investigation.

Finally, this study provides a lesson relating to the use of recombinant parasite proteins in immunological studies. Clearly recognition by antibodies against the parasite-derived protein may be insufficient to allow their use. Further analysis with respect to conformation may be warranted to ensure that unexpected immunogenicity properties are not encountered.

The authors would like to thank the Wellcome Trust (for grant 059606 to O.B., M.M.H. and others), Synergy (W.H., M.M.H. and I.B.M.) and the BBSRC (W.H. and M.M.H.) for providing funding. A.S. and O.B. are thankful to ELLETRA (Sinchrotrone de Trieste, Italy) for a beamtime award for this study.

REFERENCES

Ackerman, C. J., Harnett, M. M., Harnett, W., Kelly, S., Svergun, D. I. and Byron, O. (2003). 19 Å solution structure of the filarial nematode immunomodulatory protein, ES-62. *Biophysical Journal* **84**, 489–500.

Alcocer, M. J., Murtagh, G. J., Bailey, K., Dumoulin, M., Meseguer, A. S., Parker, M. J. and Archer, D. B. (2002). The disulphide mapping, folding and characterisation of recombinant Ber e 1 and SFA-8, two sulphur-rich 2S plant albumin allergens. *Journal of Molecular Biology* **324**, 165–175.

Ausubel, F. M., Brent, R., Kingston, R. E., Moore, D. D., Seidman, J. G., Smith, J. A. and Struhl, K. (2001). *Current Protocols in Molecular Biology*, John Wiley and Sons, New York, USA.

Chen, Z. and Ruffner, D. E. (1998). Amplification of closed circular *DNA in vitro*. *Nucleic Acids Research* **26**,1126–1127.

Durchschlag, H. (1986). Specific volumes of biological macromolecules and some other molecules of biological interest. In *Thermodynamic Data for Biochemistry and Biotechnology* (ed. Hinz, H.-J.), pp. 45–128. Springer Verlag, Berlin-Heidelberg-NewYork-Tokyo.

Geyer, R., Geyer, H., Kühnhardt, S., Mink, W. and Stirm, S. (1982). Capillary gas-chromatography of methylhexitol acetates obtained upon methylation of N-glycosidically linked glycoprotein oligosaccharides. *Annals of Biochemistry* **121**, 263–274.

Goodridge, H. S., Deehan, M. R., Harnett, W. and Harnett, M. M. (2005). Subversion of immunological signalling by a filarial nematode phosphorylcholine-containing secreted product. *Cellular Signalling* **17**,11–16.

Goodridge, H. S., Marshall, F. A., Wilson, E. H., Houston, K. M., Liew, F. Y., Harnett, M. M. and Harnett, W. (2004). *In vivo* exposure of murine dendritic cell and macrophage bone marrow progenitors to the phosphorylcholine-containing filarial nematode glycoprotein ES-62 polarizes their differentiation to an anti-inflammatory phenotype. *Immunology* **113**, 491–498.

Grinna, L. S. and Tschopp, J. F. (1989). Size distribution and general structural features of N-linked oligosaccharides from the methylotrophic yeast, *Pichia pastoris*. *Yeast* **5**, 107–115.

Harnett, W., Deehan, M. R., Houston, K. M. and Harnett, M. M. (1999). Immunomodulatory properties of a phosphorylcholine-containing secreted filarial glycoprotein. *Parasite Immunology* **21**, 601–608.

Harnett, W. and Harnett, M. M. (1993). Inhibition of murine B cell proliferation and down-regulation of protein kinase C levels by a phosphorylcholine-containing filarial excretory-secretory product. *Journal of Immunology* **151**, 4829–4837.

Harnett, W. and Harnett, M. M. (2001). Modulation of the host immune system by phosphorylcholine-containing glycoproteins secreted by parasitic filarial nematodes. *Biochimica et Biophysica Acta*. **1539**, 7–15.

Harnett, W., Harnett, M. M. and Byron, O. (2003). Structural/functional aspects of ES-62-a secreted immunomodulatory phosphorylcholine-containing filarial nematode glycoprotein. *Current Protein and Peptide Science* **4**, 59–71.

Harnett, W. Houston, K. M., Amess, R. and Worms, M. J. (1993). *Acanthocheilonema viteae*: phosphorylcholine is attached to the major

excretory-secretory product via an N-linked glycan. *Experimental Parasitology* **77**, 498–502.

Harnett, W. and Parkhouse, R. M. E. (1995). *Perspectives in Nematode Physiology and Biochemistry* (ed. Sood, M. L.), pp. 207–242. M/S Narendra Publication House, New Delhi.

Harnett, W., Worms, M. J., Kapil, A., Grainger, M. and Parkhouse, R. M. E. (1989). Origin, kinetics of circulation and fate *in vivo* of the major excretory-secretory product of *Acanthocheilonema viteae*. *Parasitology* **99**, 229–239.

Haslam, S. M., Khoo, K. H., Houston, K. M., Harnett, W., Morris, H. R. and Dell, A. (1997). Characterisation of the phosphorylcholine-containing N-linked oligosaccharides in the excretory-secretory 62 kDa glycoprotein of *Acanthocheilonema viteae*. *Molecular and Biochemical Parasitology* **85**, 53–66.

Hennessey, J. P. J. and Johnson, W. C. JR. (1981). Information content in the circular dichroism of proteins. *Biochemistry* **20**, 1085–1094.

Houston, K. M. and Harnett, W. (1999*a*). Attatchment of phosphorylcholine to a nematode glycoprotein *Trends in GlycoScience and Glycotechnology* **11**, 43–52.

Houston, K. M. and Harnett, W. (1999*b*). Mechanisms underlying the transfer of phosphorylcholine to filarial nematode glycoproteins – a possible role for choline kinase. *Parasitology* **118**, 311–318.

Houston, K. M., Cushley, W. and Harnett, W. (1997). Studies on the site and mechanism of attachment of phosphorylcholine to a filarial nematode secreted glycoprotein. *Journal of Biological Chemistry* **272**, 1527–1533.

Houston, K. M., Wilson, E. H., Eyres, L., Brombacher, F., Harnett, M. M., Alexander, J. and Harnett, W. (2000). Presence of phosphorylcholine on a filarial nematode protein influences immunoglobulin G subclass response to the molecule by an interleukin-10-dependent mechanism. *Infection and Immunity* **68**, 5466–5468.

Kurniawan, A., Yazdanbakhsh, M., Van Ree, R., Aalberse, R., Selkirk, M. E., Partono, F. and Maizels, R. M. (1993). Differential expression of IgE and IgG4 specific antibody responses in asymptomatic and chronic human filariasis. *Journal of Immunology* **150**, 3941–3950.

Johnson, M., Correia, J. J., Yphantis, D. A. and Halvorsen, H. (1981). Analysis of data from the analytical ultracentrifuge by nonlinear least square techniques. *Biophysical Journal* **36**, 575–588.

Lamm, O. (1929). Die Differentialgleichung der Ultrazentrifugierung. *Arkiv för Matematik, Astronomi och Fysik* **21B**, 1–4.

Laue, T. M., Shah, B. D., Ridgeway, T. M. and Pelletier, S. (1992). Computer-aided interpretation of analytical sedimentation data for proteins. In *Analytical* Ultracentrifugation in Biochemistry and Polymer Science (ed. Harding, S. E., Rowe, A. J. and Horton, J. C.), pp. 90–125. Redwood Press Ltd, Melksham.

Lawrence, R. A. (2001). Immunity to filarial nematodes. *Veterinary Parasitology* **100**, 33–44.

Maizels, R. M., Blaxter, M. L. and Scott, A. L. (2001). Immunological genomics of *Brugia malayi*: filarial genes implicated in immune evasion and protective immunity. *Parasite Immunology* **23**, 327–344.

Ottesen, E. A., Skvaril, F., Tripathy, S. P., Poindexter, R. W. and Hussain, R. (1985). Prominence of IgG4 in the IgG antibody response to human filariasis. *Journal of Immunology* **134**, 2707–2712.

Provencher, S. W. and Glockner, J. (1981). Estimation of globular protein secondary structure from circular dichroism. *Biochemistry* **6**, 33–37.

Schuck, P. (1998). Sedimentation analysis of noninteracting and self-associating solutes using numerical solutions to the Lamm equation. *Biophysical Journal* **75**, 1503–1512.

Schuck, P. (2000). Size-distribution analysis of macromolecules by sedimentation velocity ultracentrifugation and Lamm equation modeling. *Biophysical Journal* **78**, 1606–1619.

Schuck, P. (2004). Sedimentation equilibrium analysis of protein interactions with global implicit mass conservation constraints and systematic noise decomposition. *Analytical Biochemistry* **326**, 234–256.

Schuck, P., Perugini, M. A., Gonzales, N. R., Howlett, G. J. and Schubert, D. (2002). Size-distribution analysis of proteins by analytical ultracentrifugation: strategies and application to model systems. *Biophysical Journal* **82**, 1096–1111.

Sreerama, N. and Woody, R. W. (1993). A self-consistent method for the analysis of protein secondary structure from circular dichroism. *Analytical Biochemistry* **209**, 32–44.

Stepek, G., Auchie, M., Tate, R., Watson, K., Russell, D. G., Devaney, E. and Harnett, W. (2002). Expression of the filarial nematode phosphorylcholine-containing glycoprotein, ES-62, is stage specific. *Parasitology* **125**, 155–164.

Subramanian, S., Stolk, W. A., Ramaiah, K. D., Plaisier, A. P., Krishnamoorthy, K., van Oortessen, G. J., Dominic Amalraj, D., Habbema, J. D. and Das, P. K. (2004). The dynamics of *Wuchereria bancrofti* infection: a model-based analysis of longitudinal data from Pondicherry, India. *Parasitology* **128**, 467–483.

Volkov, V. V. and Svergun, D. I. (2003). Uniqueness of *ab initio* shape determination in small-angle scattering. *Journal of Applied Crystallography* **36**, 860–864.

Whitmore, L. and Wallace, B. A. (2004). DICHROWEB, an online server for protein secondary structure analyses from circular dichroism spectroscopic data. *Nucleic Acids Research* **32**, W668–W673.

World Health Organization (1997). Prospects for the elimination of some TDR diseases. *World Health Organization*, *Geneva*.

Wilson, E. H., Deehan, M. R., Katz, E., Brown, K. S., Houston, K. M., Orquote Grady, J., Harnett, M. M. and Harnett, W. (2003). Hyporesponsiveness of murine B lymphocytes exposed to the filarial nematode secreted product ES-62 *in vivo*. *Immunology* **109**, 238–245.

Yphantis, D. A. (1960). Equilibrium ultracentrifugation of dilute solutions. *Biochemistry* **3**, 297–317.